Journal of Cleaner Production 279 (2021) 123511

Contents lists available at ScienceDirect

Journal of Cleaner Production

journal homepage: www.elsevier.com/locate/jclepro

Exergy analysis of a pilot-scale reactor using wood chips

Alok Dhaundiyal [a, *], Divine Atsu [a, b]

[a] Institute of Process Engineering, Szent Istvan University, Godollo, 2100, Hungary
[b] Koforidua Technical University, Box 981, Koforidua, Ghana

ARTICLE INFO

Article history:
Received 15 March 2020
Received in revised form
24 July 2020
Accepted 26 July 2020
Available online 12 August 2020

Handling editor: Bin Chen

Keywords:
Exergy
Reactor
Thermal
Pyrolysis
Biomass
Energy loss

ABSTRACT

A pilot size reactor has been tested to examine the suitability of the design for effective gas generation. The qualitative assessment of a reactor is considered to be one of the selection criteria for the thermochemical conversion. The pyrolysis reactor is subjected to operate for the temperature histories of 32 −400 °C and 33−600 °C, respectively. The chemical exergy and the thermal efficiency are calculated for both operating ranges. The thermal efficiency of the reactor is found to be 46.32%; whereas the chemical exergy of the raw gas is 75.77% while pyrolysing at 600 °C, which is relatively 17% higher than that obtained at 400 °C. The additional burden on the thermal system due to the moisture has reduced the thermal efficiency of the reactor by 5.85% at 600 °C, whereas it is 6.22% for carrying out thermal decomposition at 400 °C. The gas yield for the given reactor is decreased by 0.77% while operating at 400 °C, whereas the char yield is increased by 6.73%. The proposed design is more efficient for higher temperature regimes and for dried biomass. The lumped system analysis is adopted to determine the loss for the transient condition. The heat transfer in the transient condition is measured for the fixed bed of biomass by the Biot and the Fourier numbers. The external heat transfer controls the overall rate of reaction. The intraparticle temperature is homogenous throughout the process though it may depend on the external heat condition. Furthermore, the various losses encountered during pyrolysis make the system energy-intensive. The objective of this work is to provide a clean generation of energy, which can be attained by improving exergetic content of the reactor.

1. Introduction

The perspective of exergy analysis of a thermal system is to assess its distinction in the energy conversion or distribution processes by determining its inaccessibility owing to the thermodynamic irreversibility. The thermo-chemical conversion process requires a system that can be efficient to exploit the exergonic ability of the fuel. The system must be effective enough to bolster propagation of the flame front and assist the decomposition of the fuel into a useful product. The exergy can either be chemical or physical, but in the case of gas production, the chemical exergy plays a significant role to determine the qualitative aspect of the system. Since the energy fluxes in the control volume is also a function of the mole fraction of constituents in the mixture which changes with time and temperature and so is the anergy of the control volume.

Pyrolysis is one of the thermochemical processes which is carried out in the absence of the oxygen, converts the fuel into the gaseous products, and bio-fuel through the shift reactions. For performing energy conversion, the reactor should be efficient enough so that the incremental heat rate matches with the ancillaries of the plant. Apart from the constructional design of the reactor, the fuel being used affects the heating value of the produced gas. The physiochemical characteristics of the fuel influence not only the transportation of energy fluxes across the control surface but also the external energy required to carry out the process. It has been reported that the moisture content of the fuel increases the burden on a 120-kW gasifier unit by 37.72 kJ kg^{-1} at the operating condition of 600−800 °C (Dhaundiyal and Gupta, 2014). Similarly, in another study, with an increased moisture content of Municipal Solid Waste (MSW) by 13.1%, the corresponding reduction in the heating value of the gas is 4.2% (Dong et al., 2016). During the thermal decomposition of trommel fines, the conversion efficiency of the pyrolysis reactor is decreased by 10% with the increase in the moisture content of trommel by 4% (Eke et al., 2019). It has also been reported that char yield is also

* Corresponding author.
E-mail address: alok.dext@hotmail.com (A. Dhaundiyal).

https://doi.org/10.1016/j.jclepro.2020.123511

Notation

A_R	A fraction of ash in residue
α_w	Thermal diffusivity of wood $m^2.s^{-1}$
B_i	The Biot number
C_R	A fraction of carbon in residue
C_{ab}	A fraction of carbon used in pyrolysis
C_f	A fraction of carbon in the gas
C_{pg}	Specific heat of gas $kJ.kg^{-1}.K^{-1}$
C_{wb}	Specific heat of wood $kJ.kg^{-1}.K^{-1}$
ε	Chemical exergy $MJ.kg^{-1}$
ε	Voidage of bed
F_0	The Fourier number
ΔG_0	Exergy input kW
$-\Delta H_0$	Enthalpy of formation kW
h	Heat transfer coefficient $W.m^{-2}.K^{-1}$
$\dot{I}_l$	The rate of exergy loss through insulation kW
$\dot{I}_e$	The rate of exergy loss in exhaust kW
$\dot{I}_d$	The rate of exergy loss in the pyrolysis kW
$\dot{I}_c$	The rate of exergy loss due to the quenching effect of medium kW
k_w	Thermal conductivity of wood $W.m^{-1}.K^{-1}$
L_c	Characteristic Length m
p_{0i}	Pressure at outlet of nitrogen cylinder bar
Q_i	Thermal losses $kJ.kg^{-1}$
r_c	Critical radius m
$\varnothing$	Exergy ratio
ρ_s	Material density $kg.m^{-3}$
ρ_b	Bulk density $kg.m^{-3}$
$T\Delta S_0$	The rate of exergy loss in reaction kW
w_g	The flow rate of gas per second $kg.s^{-1}$
w_f	Biomass consumption per second $kg.s^{-1}$
w_{N_2}	Flow rate of nitrogen $m^3.s^{-1}$
W_d	Dry producer gas per kg of fuel

reduced with increasing moisture content of the wood chips in a pyrolysis reactor (Burhenne et al., 2013). Though a higher yield of gas is obtained at higher pyrolysis temperature (800 °C) it is independent on the initial water content of the wood (Di Blasi, 2009). It has been reported that a percentage decrease in the moisture of the biomass enhance the exergy of the system by nearly 1 GJ ha^{-1} (Soto and Romanelli, 2020).

Apart from the effect of moisture content on the energy of the system, the exergetic aspect of the thermal boundary cannot be overlooked to investigate the carbon conversion. It has been reported that biomass with higher carbon content and lower ash content increases the exergy efficiency of the gasifier (Rupesh et al., 2016). Kabalina et al. (2017) has carried out the exergy analysis of a polygeneration system and they have concluded that the retrofitting SNG units with a gasifier reactor would improve the overall performance of the unit, as well as the exergy of the reactor, whiles reducing the products exergoeconomic costs (Kabalina et al., 2017). Li et al. (2019) investigated the agglomerating fluidised bed (AFB) gasification using the Aspen plus. They have reported that the increasing carbon conversion might reduce the exergy destruction in the AFB gasifier. It has been concluded that the intensive properties of the system affect the exergy analysis. The increasing temperature and pressure reduce the anergy level of the system. They managed to save 54.18% exergy loss using the AFB in place of a fixed bed gasifier (Karamarkovic and Karamarkovic, 2010). As they have mentioned, the carbon conversion is one of the significant factors to measure imperfections of the system due to the thermodynamic irreversibility. Therefore, the carbon boundary point should have been addressed for the AFB unit. The carbon boundary point is defined as the critical level of oxygen that can be supplied without lowering the heating value of the producer gas in a gasifier. During gasification of feedstocks having different moisture content, it has been concluded that the gasification of biomass above the temperature at the carbon boundary point could increase the moisture of the biomass, which consequently, reduces the energy and exergy of the produced gas. It is recommended that the dried biomass is beneficial for improving the chemical energy and exergy of the air-blown biomass gasifier (Karamarkovic and Karamarkovic, 2010). This CBP can be obtained if adequate gasifying medium is provided to prevent carbon formation and achieve the complete gasification (Karamarkovic and Karamarkovic, 2010). Other researchers have also confirmed that the CBP is the optimum point for demarcating the peak change in enthalpy of the system (Prins et al., 2003; Double and Bridgewater, 1985). For a typical gasification process, the equivalence ratio lies in the domain of $0.3 < \varphi < 0.4$, but in case of pyrolysis, it is $\varphi \sim 0$, therefore the exergy of a gas predominately depends on the intensive properties of the reactor.

The main objective of this study is to investigate a pilot scale reactor for gas production and to make an efficient generation of energy without disturbing the equilibrium of the environment. The qualitative effectiveness and the areas which increase exergy destruction are identified so that the desired pyrolysis unit can be implemented for industrial purposes. The temperature distribution is unsteady, and it varies point-to-point; thus, it becomes necessary to implement the lumped heat transfer model so that the analysis can be simplified. The thermal time constant is also calculated for the unit to know the response time for a change in its ambient temperature.

2. Material and methods

A small-scale pyrolysis reactor has been chemically as well as thermally examined. The exergy analysis of has been conducted for the gas generation. The exergy of the system, along with the thermal losses encountered along with the production of gas, has been calculated with the help of first and second laws of thermodynamics. The application of heat-transfer to determine the effect of temperature on the system performance has been studied in the subsequent sections.

2.1. Exergy analysis of the system

The exergy of a system is the maximum work obtainable as the system comes to equilibrium with its surroundings (Bejan, 2016). The effectiveness of the reactor can be known by the qualitative assessment of the energy generated during the thermochemical conversion. The first law of thermodynamics provides an insight into the energy balance between the system and the surrounding. It does not demarcate the different forms of energy, especially between work and heat, or the internal energy available at different temperatures. It is a law of degradation of energy or law of entropy that asserts from the engineering stance all the forms of energy that are not of the same quality. It may be possible that the energies of

the two systems are quantitively equal, but they may vary qualitatively. The perfectness of any thermal system is determined by the exergetic efficiency, whereas the availability/inaccessibility of energy is determined by the exergy analysis. The energy of the system remains constant, but the exergy is always destroyed. The advantage of exergy analysis is that it provides information about the exergy loss or irreversibility in the sub-units, which contributes to the overall energy assessment of the power plant. This can be attained by thermodynamically optimising the operating or geometrical parameters, so as to reduce the values to practical minimum values.

For dry fuels, the exergy ratio ($\varnothing$) of the chemical exergy of the fuel and the net calorific value (N.C.V) is given by (Kotas, 1985)

$$\varnothing = \frac{1.0437 + 0.1182\left(\frac{H}{C}\right) - 0.2509\left(1 + 0.7256\left(\frac{H}{C}\right) + 0.0383\left(\frac{N}{C}\right)\right)}{1 - 0.3035\left(\frac{O}{C}\right)} \tag{1}$$

equation (1) is valid for the mass ratio of. $0.667 < \frac{O}{C} < 2.67$

For the chemically reactive system,

$$\varepsilon = \frac{-\Delta G_0}{-\Delta H_0} \tag{2}$$

Therefore, ΔG_0 can be estimated.

Again,

$$\Delta G_0 = \Delta H_0 - T_0 \Delta S_0 \tag{3}$$

$$\Delta H_0 = w_f\ (NCV)_0\ (\text{kW}) \tag{4}$$

Here,

$$T_0 \Delta S_0 = \text{rate of exergy loss inpyrolysis} = w_f\ (NCV)_0 (\varnothing - 1)(\text{kW}) \tag{5}$$

The rate of dissipation of energy during decomposition of the wooden chips

$$\dot{I}_d = T_0 \left[\Delta S_0 + w_g C_{pg} ln\left(\frac{T_i}{T_0}\right) - w_g R_g ln\left(\frac{p_i}{p_0}\right) - w_a C_{pa} ln\left(\frac{T_i}{T_0}\right) + w_a R_a ln\left(\frac{p_i}{p_0}\right) \right]\ (\text{kW}) \tag{6}$$

The rate of loss of exergy while flowing the gases through the exhaust duct

$$\dot{I}_e = w_g C_{pg} \left[(T_i - T_0) - T_0 ln\left(\frac{T_i}{T_0}\right) \right] (\text{kW}) \tag{7}$$

The rate of exergy loss during the quenching effect caused by the flow of nitrogen in a system

$$\dot{I}_c = T_{0i} \left[w_{N_2} C_{pN_2} ln\left(\frac{T_i}{T_{0i}}\right) - w_{N_2} R_{N_2} ln\left(\frac{p_i}{p_{0i}}\right) \right] (\text{kW}) \tag{8}$$

$$\eta_{II} = 1 - \frac{\sum_{i=1}^{N} \dot{I}_i}{\Delta G} = \frac{\dot{A}_{out}}{\dot{A}_{in}} \tag{9}$$

2.2. Experimental set-up

Thermal testing is conducted at the National Agricultural Research and Innovation Centre, Hungary. The G50 hardwood chip (ONORM, Austrian Standard) is used for the experimental purpose. To measure the extensive and intensive properties of the system, the temperature sensors are placed along the vertical axis of the reactor. The temperature sensors are positioned 80 mm apart from each other. The temperature sensor S-A and S−B (Fig. 1) are used to determine the temperature of the fixed bed. On the other hand, the S−C and S-D are provided to measure the temperature of the generating gas. The weight sensor is kept under the grate, which is marked by S−I. G in Fig. 1. The 'K' type (Nickel−Chromium/Nickel-Alumel) thermocouple is used to measure the temperature of the wood chips, as well as the volatile gas. The strain gauge (HBM, Germany) embedded in the surface plate has been calibrated with 500 g of iron weight before installing into the system for measuring the instantaneous mass of the woodchip with time. Pyrolysis of the wooden chips has been performed at 400 °C and 600 °C. The upper limit of the temperature has been set according to the heating capacity of the heating filament, whereas the lower limit is a feasible limit for the pyrolysis.

The pressure sensor placed on the testing rig of the reactor is used to record the pressure variations inside the reactor. All the sensors are connected to the computer via a multi-operating-data logger (HBM, Germany). The volumetric rate of the inert gas is controlled and measured by a pressure regulator and a gas meter (Ganz, Budapest, Hungary), respectively. The maximum volumetric capacity of the gas meter is 7.57 $m^3\ min^{-1}$. The indirect heating to the system is provided by a heating element (Pelletstar, Herz, Germany). The rated capacity of the heating element used for the indirect heating of the reactor is 2 kW (Fig. 2(b)). The material used for a grate fabrication is 0.7 mm thick stainless-steel wire mesh. To insulate the reactor, the 50 mm thick heating resisting material, rock wool, is used to separate the reactor from the outer casing. The core of the reactor is manufactured of 1.5 mm welded carbon steel. The inner diameter of the reactor is 110 mm, while the surface diameter is 210 mm. The outer casing of the reactor is made of Aluminium foil. The schematic diagram of the pyrolysis test rig is shown in Fig. 2. Nitrogen is allowed to flow at the rate of 0.7 L s^{-1} during the experimentation. The outlet pressure of the nitrogen is set to 1.5 bar.

The elementary composition of the raw material is calculated by the CHNO−S analyser (Vario MACRO cube, Germany). The analyser is heated up to 1473 K for 30 min. Once it obtains the pre-combustion temperature required for the given material, the capsule-form of the sample is fed into the rotating disk. Tungsten trioxide VI (WO_3) has been used to oxidise the carbon and hydrogen, which are later mixed with the helium (He) gas. The function of the carrier gas (He) is to scavenge the product of combustion to different reduction columns. These tubes are located between the combustion chamber and the signal-processing unit. The components of the gas are separated by the purge or trap chromatography. Each component is individually detected by a thermal conductivity detector (TCD). The product of the combustion is absorbed in sequence, however N_2 gas does not pass through columns. The standard operating condition is based on the sample of birch leaf. The calorific value is calculated by the constant volume bomb calorimeter (IKA- WERKE C2000 basic, Germany). The ash melting point is determined by using the heating microscope optical bench, EM301, manufactured by the Hesse Instruments (Germany). The optical bench comprises the halogen lamp with condenser, the furnace mounting, and the CCD camera. The measuring cell inside the furnace is made up of the quartz glass discs. The physiochemical characteristic of the hardwood (acacia) is provided in Table 1. The composition of the gas is determined by the gas analyser, as illustrated in Table 2. The physical characteristic of G50 chips is provided in Table 3. The thermal and physical

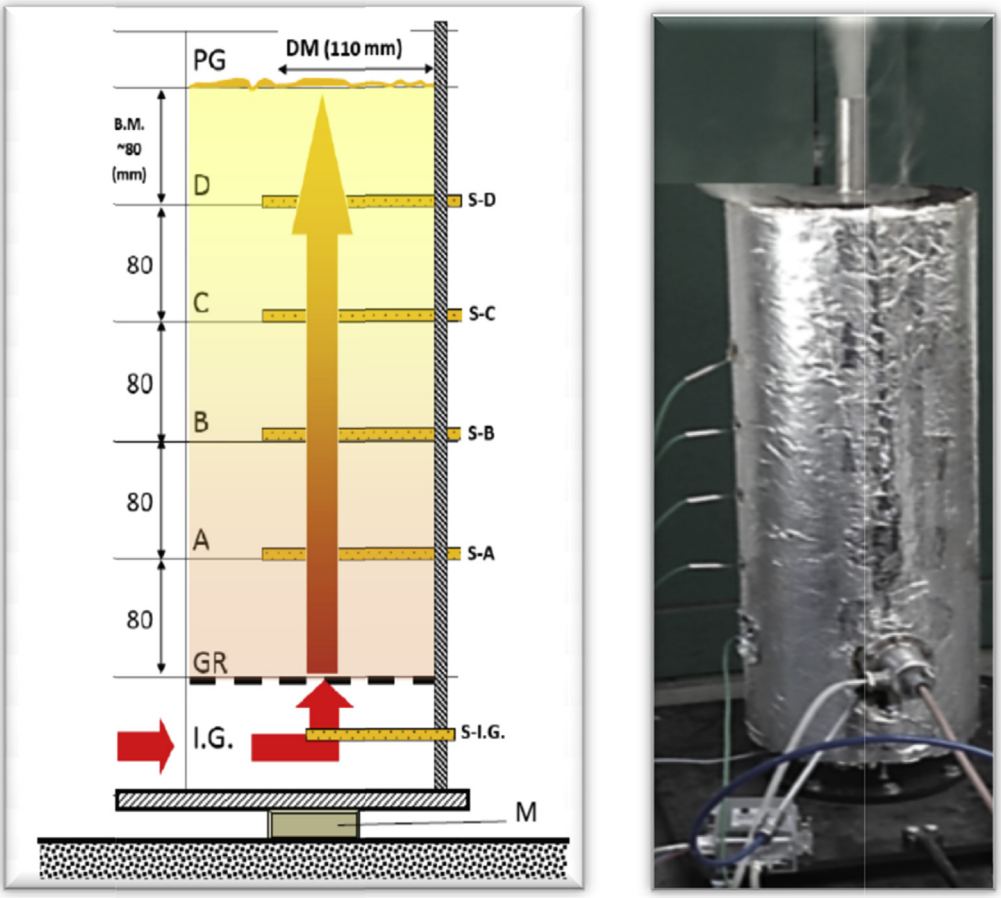

Fig. 1. Schematic diagram of the reactor showing the temperature sensors locations.

characteristic of the pyrolyzed bed is given in Table 4. It is assumed that the gas would flow along the vertical axis (updraft) of the reactor.

2.3. Thermal analysis

The effectiveness of a reactor is based on its conversion efficiency. How efficiently a system converts the chemical exergy of a fuel into electrical energy via thermochemical conversion is the main objective of any plant manufacturing company. It is also necessary to know the characteristics of the fuel that is being used for the energy generation. The higher the percentage of moisture content or the incomplete conversion of the fuel, the lower the thermal efficiency, and it makes the system energy-intensive. However, the residual mass (Char) can be used for domestic purposes and efficiently removing it out of the reactor is also equally important. Moreover, the temperature distribution and the heating rates (slow or flash pyrolysis) are the key factors in deciding the output of the pyrolysis process. The higher heating rate or the flash/rapid/fast pyrolysis (1000 $^{\circ}C.min^{-1}$) promotes the volatile and heavy hydrocarbon oil yield. On the other hand, the low heating rate supports char production through depolymerisation and cross-linking of the aliphatic chain (Tran et al., 2013; Bergman et al., 2005).

So, the end requirement of a user is a criterion to determine the heating rate. Too high temperatures or too low temperatures inside the reactor also affects the output of the thermal system, so the temperature of the reactor should be optimised in such a way that the output can be maximised. If the temperature of the reactor is set high, an additional burden is imposed on the ancillary units of the plant. The heat transfer losses, as well as the net heat rate (NHR) of the plant, are some of the parameters which are affected by the temperature distribution. Apart from the performance assessment, another factor that is related to the operating temperature is the ash melting point. Therefore, it becomes indispensable to determine the ash softening temperature of the material used for energy production. The plastic flow of the ash inside the reactor impedes the gas flow and hampers the thermo-chemical process; hence, special attention is required to handle the collected ash. Among the operating conditions, the residence time of the volatile gases inside the reactor also play a crucial role in deciding the yield of the residual mass. The residence time gets minimised when the rate of heat transfer within the particle is faster than the reaction rate. It implies that the solid temperature must be essentially homogenous throughout the reactor; therefore, kinetic study is an intrinsic factor. This can be determined by calculating the Biot number or pyrolysis number for the material (Prins et al., 2006; Basu, 2016). The losses which mainly occur inside the reactor are either due to refuse or moisture content, thus relative assessment of the effectiveness of the reactor for different operating conditions, i.e. temperature and pressure (Figs. 3 and 4), is necessary.

During operation of the pilot unit, there are some losses encountered, which are evaluated through the following expressions (Nag, 2002).

Energy loss due to unburnt carbon residue

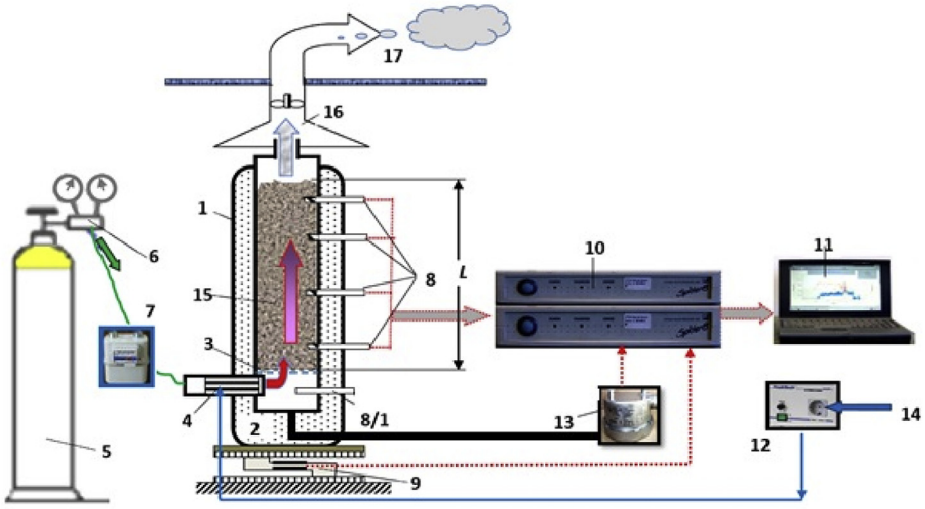

(a)

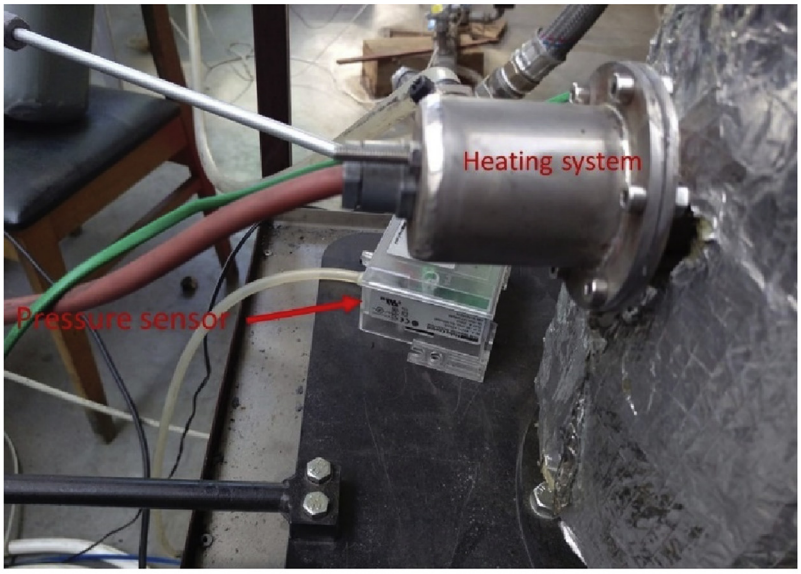

(b)

Fig. 2. (a). Schematic diagram of the pyrolysis test rig (1- Main body, 2- Insulator, 3-reactor, 4- heating element, 5- N_2 cylinder, 6- pressure valve, 7- flow meter, 8- temperature sensors, 8/1 – temperature sensor for biomass, 9 – Weight measuring sensor, 10- data logger, 11- computer, 12- heating unit, 13- Pressure sensor for reactor, 14 electrical relay, 15- feedstock, 16- chimney, 17- exhaust outlet; (b) Heating system with the pressure sensor on the test rig.

Table 1
The physiochemical composition of Hardwood (Acacia).

C %	H%	N%	O%	S%	Cl %	Ash %	[a]H.C. V (MJ/kg)	[b]N.C. V (MJ/kg)	Ash melting point (K)
50.030	5.849	0.075	42.947	0.061	0.002	1.037	19.976	18.700	1700

[a] High calorific value.
[b] Net calorific value.

Table 2
Gas composition (mass basis) (NTP).

CO %	CO_2%	H_2%	CH_4%	N_2%
16.30	21.8	1.620	1.17	59

Table 3
Physical Characteristics of the Wood chips (G50) (Onorm M 7133) (https://ec.europa.eu/energy/intelligent/projects/sites/iee-projects/files/projects/documents/forest_standards_guide_en.pdf, 2012) (CTI, 2000).

Length (m)	Cross section area (m^2)	Maximum moisture (%)	Water content class	Ash content class
0.05	**0.0005**	**22–30**	**W-30**	**A-2 (<1.5)**

Table 4
Thermal and physical properties of wood and producer gas.

C_{pg}	K_b	C_{wb}	α_w	$\in$	ρ_s	ρ_b	$r_{c,400}$	h_{400}	h_{600}	$r_{c,600}$
1.222	0.10617	0.661	0.000294	0.28	760	545	0.73	0.088	0.136	0.47

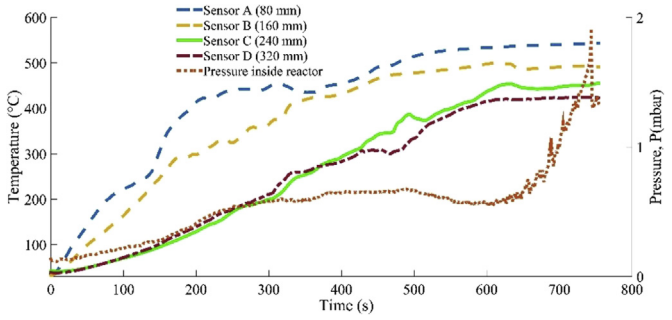

Fig. 3. Temperature and pressure variation along the height of the reactor (600 °C).

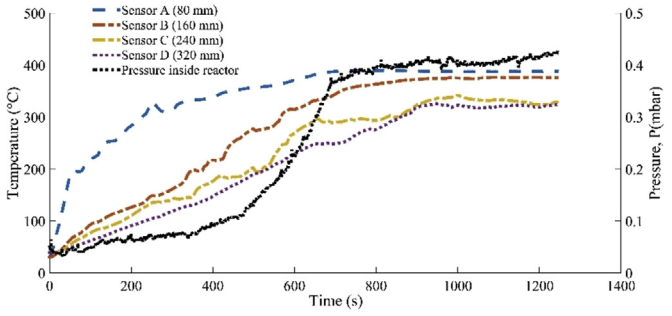

Fig. 4. Temperature and pressure variation along the height of the reactor (400 °C).

$$Q_1 = 33917(C - C_{ab})\text{kJ/kg} \tag{10}$$

Energy loss due to the formation of carbon monoxide (CO)

$$Q_2 = 10100\, W_d\, (CO\,/\,(CO + CH_4 + CO_2 + H_2 + N_2))\text{kJ/kg} \tag{11}$$

Energy loss due to moisture in the fuel

$$Q_3 = M\Big(4.2\Big(100 - T_f\Big) + 2256.8 + 2.09(T_g - 100)\Big)\text{kJ/kg} \tag{12}$$

Here.

T_f is the initial temperature at t ($t = 0$) and T_g denotes the final temperature at different sections of the reactor.

Energy loss due to exhaust gas

$$Q_4 = W_d\, C_{pg}(T_e - T_0) \tag{13}$$

Here, T_e is the average temperature across the bed and T_0 is the ambient temperature (288 K).

Energy loss due to hydrogen in the fuel

$$Q_5 = 9H\Big(4.2\Big(100 - T_f\Big) + 2256.8 + 2.09(T_g - 100)\Big) \tag{14}$$

Energy loss due to refuse

$$Q_6 = [(\,C - C_{ab}) + A]C_{pa}\big(T_g - T_0\big) \tag{15}$$

Energy gain by the bed due to conduction-unsteady-state (lumped system analysis) (Holman, 2010)

$$Q_7 = \frac{\rho_b V_b dT}{dt} = hA_s(T - T_0)$$

For the transient condition, the temperature distribution is given by.

$\theta = \theta_0 e^{-\frac{hA_s\tau}{\rho_b V_b}}$ or. $\theta = \theta_0 e^{-Bi\, F_0}$

Voidage of the bed can be determined by

$$\varepsilon = 1 - \left(\frac{\rho_b}{\rho_s}\right) \tag{16}$$

Here, the Biot (Bi) and the Fourier (F_0) numbers signify temperature distribution and degree of penetration of heat across the bed, respectively.

$$Bi = \frac{hL_c}{k}\ F_0 = \frac{\alpha\tau}{L_c^2}$$

where $\theta = T - T_0$ and. $\theta = T_i - T_0$

T- Temperature at time t

$$Q_7 = \frac{h\theta_0 A_s\left(\,e^{-Bi\, F_0}\right)}{w_f} \tag{17}$$

Energy loss through the rock wool insulation is given by,

$$Q_8 = \frac{(T_e - T_0)}{\frac{\sum_{n=1}^{n=k}\frac{1}{k_{n-1}}\ln\left(\frac{r_n}{r_{n-1}}\right)}{w_f}} \tag{18}$$

Balancing of elemental constituents of wood chips during the combustion and pyrolysis.

Combustion of Hardwood (Acacia) (Theoretical)

$$\frac{50.030}{12}C + \frac{5.849}{2}H_2 + \frac{42.947}{32}O_2 + \frac{0.061}{32}S + aO_2 + (h = 3.76a)N_2 \rightarrow bCO_2 + cH_2O + dSO_2 + eN_2 + fCO$$

Pyrolysis of Hardwood (Acacia) (Experimental)

$$\frac{50.030}{12}C + \frac{5.849}{2}H_2 + \frac{42.947}{32}O_2 + \frac{0.061}{32}S + h\,N_2 + aO_2 + c\,H_2O \rightarrow bCO_2 + dSO_2 + eN_2 + fCO + g\,CH_4 + kH_2$$

The stoichiometric coefficients of both reactions are given in Table 4.

3. Results and discussion

The pyrolysis of the G50 wood chips has been done at 400 °C and 600 °C, respectively. The exergy analysis of the pyrolysis reactor has been performed to calculate the change in the energy fluxes of the control volume. The external heat is provided to the unit by the heating element, which helps in initiating the pyrolysis of the hardwood chips. The losses due to change in the enthalpy of the system are determined at the four different sections (A, B, C and D) of reactor. It is illustrated in Figs. 3 and 4, respectively, that the temperature ramps from 33 °C to 600 °C and 32 °C–400 °C. However, the simultaneous flow of the nitrogen gas causes the quenching effect, so in both cases, temperature deviation of approximately 2–3 °C between the measured temperature and the temperature controller. Another reason for the fluctuation of temperature is the heat of reaction. It can be clearly understood from the combustion mechanism or Boudouard reaction (redox) that the dissociation of carbon dioxide at a higher temperature alters the Gibbs free energy of the system, which eventually influence the heat of reaction. The oxygen fraction is relatively very low in the pyrolysis process; therefore, the flame front does not have sufficient oxygen to convert carbon (C) into carbon dioxide (CO_2). It shifts the exothermic reaction into the endothermic reaction, but this phenomenon occurs at an elevated temperature. The same phenomenon can be seen while burning the coal inside the furnace (Nag, 2002).This process also affects the various losses that occur during the thermochemical conversion of the fuel into the volatile components, and it alters the chemical exergy. The Boudouard reaction may also affect the pyrolysis process as the reduction of carbon monoxide into carbon and carbon dioxide also affects the heat of reaction and the thermal efficiency of the system. For slow heating rate, the endothermic range for the wood lies at a temperature less than 250 °C, whereas, for the endothermic char surface, it lies in the domain of 340 °C–520 °C.

In the case of wood, the grain orientation with respect to the heating direction also affects the yield of char and the volatile components (Lee et al., 1977). The heating parallel to the grain orientation has a low residence time of the volatile inside the solid matrix. In this way, the effect of mass transfer is negligibly low. Due to this reason, the secondary pyrolysis reactions get impaired and consequently, the char yield as well as the heat of reaction, decrease. In an experiment on wood, it has been seen that at higher heat fluxes, the overall heat of reaction is exothermic, which is higher when the heating direction is perpendicular to the grain orientation. The reason given for this behaviour is that the pyrolysis gases have a much higher residence time in a solid matrix, which eventually increases the extent of the secondary reactions. These reactions are believed to be exothermic (Lee et al., 1977; Chan, 1985).

The pressure exponentially increases until the temperature inside the reactor reaches the saturation point of 600 °C. In contrast, there is a sudden drop in the pressure inside the reactor due to the variation in the bed regime with time. Once the incipient bed reaches the slugging stage, the pressure drop across the bed usually occurs. However, if the superficial velocity of the particles remains in-between the fluidisation velocity and the turbulent velocity of the particles, it can be averted. On the other hand, the continuous surging of temperature along the reactor causes the pressure drops succumbed. The comparative plot of the thermogravimetric variation of the hardwood chips at 400 and 600 °C is shown in Fig. 5. As it is seen through the decomposition of the mass, the curves get shifted to the left for higher operating ranges of temperature and pressure. The conversion rate is relatively faster for higher temperature intervals. This can be comprehended through the application of a heat transfer model for the transient state. Both selected operating temperatures satisfy the lumped-capacitance model conditions despite the relative variation of mass decomposition due to lower convective resistance. The higher degree of the conductive transport rate and relatively low thermal time -constant increases the decomposition and conversion rate of biomass. The residence time gets minimised when the rate of heat transfer to and within the particle is faster than the reaction rate, which happened in this case. The effect of the internal and external heat transfer and the pyrolysis kinetics in the conversion process is determined through the characteristic number, and the Pyrolysis number $\left(Py = \frac{k}{K\rho C_p L_c^2}\right)$, which is a ratio of the reaction time to the conduction time (Kung, 1972; Maa and Bailie, 1973; Pyle and Zaror, 1984), where, 'K' is the rate constant. This characteristic number is relatively low, i.e. the thermal system is guided by the heat transfer model rather than the chemical kinetic model. The system can be marked as thermally thin, where the temperature gradient within the intraparticle is negligible; however, it may be influenced by the external conditions. So, the relative importance of the external heat transfer with respect to the 'external' pyrolysis number $\left(Py' = \frac{h}{K\rho C_p L_c^2}\right)$ will dominate the pyrolysis of hardwood chips for the given design, and the internal heat transfer is no longer a deciding factor.

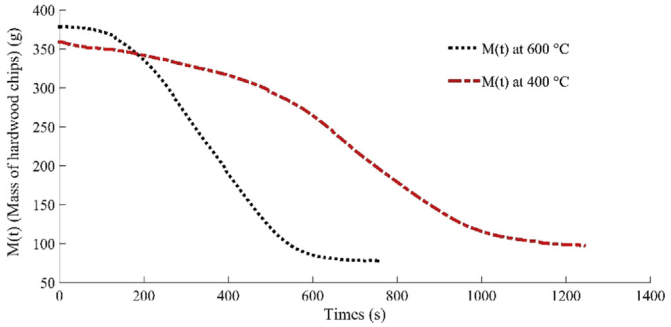

Fig. 5. Thermogravimetric variation of hardwood chips at different operating conditions.

In the reactor, carbonisation is uniform throughout the hardwood chips, and the external heat transfer controls the overall rate as the $Py' < 1$. Both operating conditions provide the uniform carbonisation, but the pyrolysis at 400 °C is relatively favourable for the char production. In addition, how quickly the thermal equilibrium is attained between the sample and environment depends on the relative rates of heat transfer to the sample (measures externally by h) and intrinsic kinetics (Pyle and Zaror, 1984).Similarly, the working procedure of a thermogravimetric analyser is quite different from the industrial reactor as the heating rate is not fixed for the industrial usage, and the pyrolysis mechanism is driven by both heat transfer and the chemical kinetic models. So, the involvement of the heating rate and the shifting of the curves due to the heat transfer limitation is omitted in this analysis.

The effect of varying temperature at different sections of the

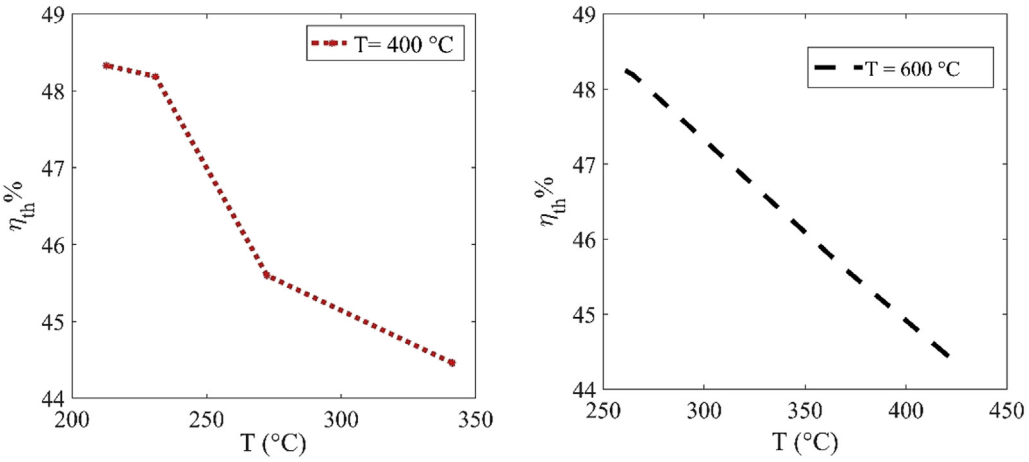

Fig. 6. Variation of thermal efficiency (η_{th}) with respect to temperature (T).

reactor on the thermal efficiency is illustrated in Fig. 6. The thermal efficiency of the reactor operated at 400 °C decreases linearly with increasing temperature of the reactor, whereas there is a marginal change in the thermal efficiency of the reactor at 600 °C in the interval of 250 °C–300 °C. Moving along the axis of the reactor, the relative increase in the thermal efficiency with the base of the reactor has found for both cases (400 °C and 600 °C). The enthalpy of the gas continuously increases with decreasing temperature of the reactor, but the overall enthalpy of the reactor is reduced by 56.72% when it is operated at 400 °C. The relative loss in energy due to the residual mass is found to be 58.36% at the lower operating range, but the overall energy saving of 0.62% is obtained while working at the operating conditions of 600 °C and 0.00056 bar. The energy loss due to the unburnt carbon and the energy gain by the bed during the pyrolysis at 400 °C are 23.09% and 11% higher than that pyrolysis occurring at 600 °C, whereas the energy loss due to carbon monoxide (CO) is 2.1% lesser at 400 °C. The heat loss through the insulator is 67% lower than the heat loss that takes place at 400 °C. The reason for this extra heat loss is that the insulation of the Rock-wool is less than the critical thickness (Table 4) required to minimise the heat loss. The critical thickness needed for maximising the thermal resistance is 55.31% higher than the critical thickness required at 600 °C, whereas an additional insulation of 363.5 mm and 623.5 mm are required to minimise the heat loss through the insulation at 600 °C and 400 °C respectively. The comprehensive details of the thermal parameters are tabulated in Tables 5, 6, 7 and 8.

The chemical composition of the species generated during the thermochemical conversion is graphically illustrated through the ternary diagram (Fig. 7.). It is visible that the reactor is suitable for pyrolysis of any material, however, the scintilla of oxygen due to its low partial pressure in the gaseous mixture might affect the pyrolysis process. The ternary plot is trifurcated (zone I, zones II and III). Zone I represents the spatial composition of the hardwood, whereas zones II and III denote the pyrolysis and combustion, respectively. It should be noted that the stoichiometric composition of the product of combustion (POC) is based on the theoretical assumption of the complete combustion so that the thermochemical process can be relatively demarcated with respect to it. The area between the zone I and the zone II denotes the fractional composition of CO and CO_2, whereas the area between the zone III and the zone I denotes the product of combustion (CO, CO_2 and H_2O). The gasification process lies between zone II and zone III (Dhaundiyal and Gupta, 2014).

The decay of the chemical energy is based on the exergy loss due to the entropy change of the system and its surrounding. Unlike the thermal losses, the degradation of the energy is relatively less and predominantly, the exergy loss during the thermochemical conversion has occurred due to the increasing entropy of nitrogen. Unlike combustion, degradation of energy is relatively low as the consumption rate is very low for both cases; however, it may increase for medium or large reactors. At the operating temperature of 600 °C, the second law efficiency(η_{II}) of the reactor varies between 74% and 77%; whereas it is 61–68% at 400 °C. Therefore, it is clear from both analyses (quantitative as well as qualitative) that the reactor must be operated at a higher temperature gradient. For the same chemical exergy (ε), the exergy input at 400 °C is 47% lower than the exergy provided at 600 °C. Although the thermal losses that occurred during the process is approximately the same for both cases, yet the overall performance can be enhanced if the operating parameters are optimised. The exergy available to carry out the thermo-chemical process is 54.66% less than the exergy-out at 600 °C. The irreversibility during the pyrolysis process occurs due to the purging effect of the nitrogen flowing along the axis of the reactor. The heat of the reaction varies drastically during the pyrolysis process, and the flow of nitrogen intensified the degradation of the exergy provided through the exothermic reactions. The detailed information of the exergy losses at the different processes is illustrated in Tables 9 and 10.

It can be concluded that the given design of the reactor is suitable for small-scale production of electricity at limited time-scale. The thermal effectiveness can be improved if the carbon conversion can be modified. The pre-treated biomass can be a boon for the pilot-size plant. The majority of energy losses are caused by the

Table 5
Stoichiometric reactions coefficient (mass basis %).

Process	a	H	b	c	d	e	f	g	k
Combustion	4.291	16.262	4.169	2.924	0.00191	16.267	0	0	0
Pyrolysis	1.6012	6.020	2.25	0.43	0.00191	6.026	1.7978	0.1212	3.22

Table 6
Flow parameters of wood, gas and inert medium (N_2).

T (°C)	w_f(kg.s^{-1})	C_f	W_{dfg}(wt. basis)	C_R	W_d(wt. basis)	C_{ab}	A_R	w_g(kg. s^{-1})	w_{N_2}(L. s^{-1})	p_{0i}(bar)
600	0.000398	0.1405	4.76	0.867	3.077	0.432	0.132	0.00233	0.7	1.5
400	0.000210	0.1405	4.76	0.8938	3.005	0.415	0.1061	0.00233	0.7	1.5

Table 7
Parametric information at different sections of the pyrolysis reactor at 600 °C (thermal losses).

Q_i	A (80 mm)	B (160 mm)	C (240 mm)	D (320 mm)
Q_1 (kJ/kg)	2408.107	2408.107	2408.107	2408.107
Q_2 (kJ/kg)	5059.706	5059.706	5059.706	5059.706
Q_3 (kJ/kg)	250	241.80	224.66	223.22
Q_4 (kJ/kg)	1519.29	1331.21	936.77	902.78
Q_5 (kJ/kg)	1666.56	1612.05	1497.74	1488.17
Q_6 (kJ/kg)	158.316	158.316	158.316	158.316
$-Q_7$ (kJ/kg)	5.577	8.7185	4.138	6.080
Q_8 (kJ/kg)	36.349	63.701	67.238	86.399
Power supplied	0.0166 kW	0.0288 kW	0.0284 kW	0.0368 kW
Fractional loss of supplied power during pyrolysis	87%	87.9%	94.21%	93.42%
$\sum Q_i$ (kJ/kg)	11,092.751	10,866.171	10,348.399	10,320.618
H.H. V (kJ/kg)	19976	19976	19976	19976
η (efficiency of pyrolysis reactor)	44.46%	45.60%	48.19%	48.33%
ΔH (kJ/kg) of gas	1515.736	1550.144	1638.18	1644
B_i	0.051	0.045	0.020	0.023
F_i	147	147	147	147
τ_{th}	75.35 s	84.67 s	188.75 s	164.98s

Table 8
Parametric information at different sections of the pyrolysis reactor at 400 °C (thermal losses).

Q_i	A (80 mm)	B (160 mm)	C (240 mm)	D (320 mm)
Q_1 (kJ/kg)	2964.345	2964.345	2964.345	2964.345
Q_2 (kJ/kg)	4952.5	4952.5	4952.5	4952.5
Q_3 (kJ/kg)	240.050	228.711	221.879	218.879
Q_4 (kJ/kg)	1196.170	943.757	791.675	724.892
Q_5 (kJ/kg)	1603.619	1527.870	1482.230	1462.189
Q_6 (kJ/kg)	65.913	65.913	65.913	65.913
$-Q_7$ (kJ/kg)	6.210	6.548	5.027	5.581
Q_8	110.330	87.049	73.021	66.861
Power supplied	0.024 kW	0.019 kW	0.016 kW	0.015 kW
Fractional loss of supplied power during pyrolysis	94.67%	93%	93.55%	92.29%
$\sum Q_i$ (kJ/kg)	11128.62	10765.066	10547.328	10451.44
H.H. V (kJ/kg)	19976	19976	19976	19976
η (efficiency of pyrolysis reactor)	44.29%	46.11%	47.20%	47.68%
ΔH (kJ/kg) of gas	648.76	680.30	700	717.83
B_i	0.037	0.025	0.015	0.014
F_i	241.336	241.336	241.336	241.336
τ_{th}	104.07 s	155.11 s	253.80 s	278.29 s

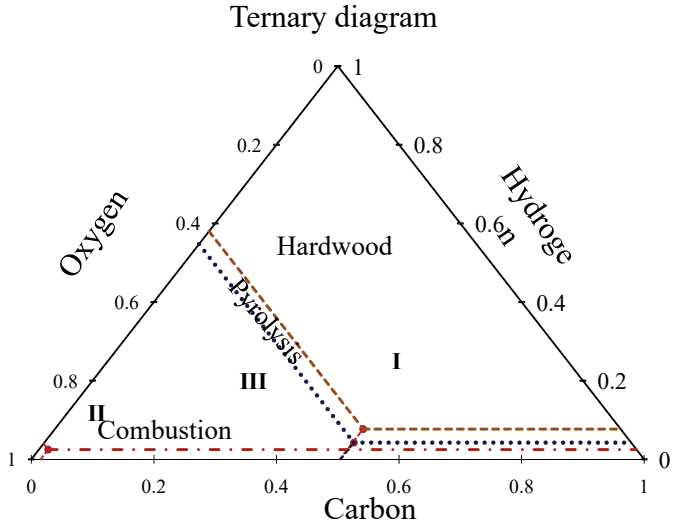

Fig. 7. Ternary diagram of chemical composition.

Table 9
Parameters related to the chemical exergy of the wooden chips.

Temperature (°C)	ε (MJ/kg)	∅	-ΔG$_0$ (kW)	TΔS$_0$ (kW)	-ΔH$_0$ (kW)
600	19.859	1.061	7.89	0.45 kW	7.44
400	19.859	1.061	4.17	0.239 kW	3.930

high fraction of the residual biomass, the formation of CO, the hydrogen content of the fuel, the unprocessed exhaust gas, and the moisture content. However, the losses due to the high hydrogen content of the fuel and the formation of CO during the process largely depend upon the chemical composition of the fuel and the thermochemical conversion efficiency, respectively. Out of 50.03% carbon in the hardwood, it is found that the average 14% of carbon is converted into the gaseous products, while 86% carbon is either unprocessed or converted into char and ash. The given design is more suitable for bio-char yield than the oil yield as it is more cost-effective to operate the small-scale reactor for domestic usage than for industrial purposes. The char yield for the given reactor at the pyrolysis temperature of 400 °C is 27.20%, whereas it is 20.47%

Table 10
Chemical exergy of the produced gas.

$\dot{I}_i$	600 °C				400 °C			
	A	B	C	D	A	B	C	D
$\dot{I}_d$ (kW)	0.6949	0.6979	0.6327	0.6013	0.3977	0.3839	0.2914	0.2883
$\dot{I}_e$ (kW)	0.5060	0.5098	0.4235	0.3812	0.3407	0.3253	0.2571	0.2340
$\dot{I}_l$ (kW)	0.0144	0.02535	0.0267	0.0343	0.02319	0.01829	0.01534	0.01405
$\dot{I}_c$ (kW)	0.796	0.778	0.766	0.755	0.8276	0.8228	0.8034	0.8013
$\sum \dot{I}_i$	2.0112	2.0110	1.8489	1.7718	1.5891	1.5502	1.3672	1.3376
η_{II}	74.50%	74.51%	76.56%	77.54%	61.89%	62.82%	67.21%	67.92%
Exergy out (kW)	5.87	5.88	6.04	6.11	2.5809	2.6198	2.8028	2.8324

Table 11
The variation of gas and char yield with operating temperature.

Parameter	400 °C	600 °C
Gas yield	**11.38%**	**12.15%**
Char yield	**27.20%**	**20.47%**

while operating the reactor at 600 °C. The gas yield for the given reactor is estimated to be 11.38% at a temperature range of 400 °C, whereas it is 12.15% at 600 °C (Table 11). It is clear from the analysis that the gas yield increases with increase in the temperature, whereas it is reverse for the char formation.

In an experiment conducted by He et al. (2010), the syngas is produced through an MSW fixed-bed reactor, and it is found that the increasing gas yield directly correlates with the temperature of the reactor. In a similar case, 76.64% of syngas is generated through the plasma pyrolysis reactor (Tang and Huang, 2005). As the residence time of the volatile content is relatively low in this reactor, the extent of the secondary pyrolysis is lower than that of the medium and large-scale reactor, therefore the reactor is very promising for small-scale electrification. The depolymerisation and the cross-linking will be limited for a high-temperature range and thin specimen conditions. It is also noted that the higher temperature favour tar decomposition and the thermal cracking of tar to increase the yield of syngas which in turn affects the oil and char yield (He et al., 2010). For the given design, the residence time of volatile falls in the domain of $5.33 > t > 2.72$. The perspective is that the small-scale reactor is very suitable for charcoal production and torrefaction process. Since thermal constraint does not allow higher gas production and even if the geometry of small-scale unit is improvised, the ratio of the cost of production of gas to the cost of fuel would be very high. However, according to economic scheduling principle, the incremental heat rate of the reactor must be comparable to the incremental heat rate of produced gas so that the cost of fuel consumption can be minimised.

4. Conclusion

A pilot-size reactor has been qualitatively and quantitatively investigated for different operating ranges, and it is critically examined whether the lower operating ranges of temperature affects the performance of the thermal system or not. According to the exergy analysis and the thermal evaluation, it is found that the small-scale reactor is not suitable for the lower range of temperatures. The valorisation of the plant has been obtained for the high-scale operating range. The thermal efficiency of the reactor for pyrolysis of the wooden chips at 600 °C is estimated to be 46.64%, which is 0.32% higher than that obtained at 400 °C. The average carbon conversion efficiency of the reactor is found to be 29%. The char yield for the given design is decreased by 6.73% with the increase in the temperature of the reactor by 200 °C. The exergy analysis also indicates that the operating range must be optimised to enhance the qualitative yield of the reactor. The gas yield of the reactor increased by 0.77% when the reactor temperature is elevated by 200 °C. There must be a 363.5 mm of additional insulation to minimise the heat-loss at an operating temperature of 600 °C. The pre-treated biomass can assist in improving the heat losses that occurred due to the energy-intensive processes (dehydration and the formation of CO).

The Biot and the Fourier numbers are also determined to know the influence of the heat and mass transfer on the pyrolysis process. The thermochemical process is governed by the external heat-transfer; thus, the rate of decomposition would be virtually instantaneous, and the sample temperature remains uniform. The exergetic efficiency of the reactor is found to vary from 66% −77%. Furthermore, the volumetric flow of the purge gas affects the exergy output of the plant. Therefore, the flow rate of nitrogen should be in proportion to the temperature of the reactor. The functioning of the reactor is suitable for a limited time scale and a higher temperature range. The major physical challenge posed by the small-scale rector is to determine the operating condition of the reactor. For the given design, the maximum operating limit is 600 °C. Since the higher thermal range can only be effective if the geometry of the reactor commensurate with the physical characteristics of the biomass. It has been found during the analysis that the electrical mode of supplying energy is not as successful as it should be since thermal diffusivity of an electrical filament does not keep up with the higher thermal history. Therefore, it has been suggested to integrate the unit with another CHP system. For cleaner energy production, the emission of CO_2 can be minimised if the unit operates at higher temperature range and in the absence of the inert medium. The exergetic output can be enhanced if the thermal gradient remains steady with time.

CRediT authorship contribution statement

Alok Dhaundiyal: Conceptualization, Methodology, Software, Writing - original draft, Formal analysis, Writing - review & editing. **Divine Atsu:** Writing - review & editing.

Declaration of competing interest

The authors declare that they have no known competing financial interests or personal relationships that could have appeared to influence the work reported in this paper.

Acknowledgement

The authors expression their sincere gratitude to NAIK-Mezőgazdasági Gépesítési Intézet, Hungary, for providing the logistics assistance.

References

Basu, P., 2016. Biomass gasification, pyrolysis and torrefaction, biomass gasification. Pyrolysis and Torrefaction. https://doi.org/10.1016/c2011-0-07564-6.

Bejan, A., 2016. Advanced Engineering Thermodynamics, Advanced Engineering Thermodynamics. https://doi.org/10.1002/9781119245964.

Bergman, P.C. a, Boersma, a R., Zwart, R.W.R., Kiel, J.H. a, 2005. Torrefaction for biomass co-firing in existing coal-fired power stations. Energy Res. Cent. Netherlands ECN ECNC05013 71.

Burhenne, L., Damiani, M., Aicher, T., 2013. Effect of feedstock water content and pyrolysis temperature on the structure and reactivity of spruce wood char produced in fixed bed pyrolysis. Fuel 107, 836–847. https://doi.org/10.1016/j.fuel.2013.01.033.

Chan, W.C.R., Kelbon, M., Krieger, B.B., 1985. Modelling and experimental verification of physical and chemical processes during pyrolysis of a large biomass particle. Fuel 64, 1505–1513. https://doi.org/10.1016/0016-2361(85)90364-3.

Dhaundiyal, A., Gupta, V.K., 2014. The analysis of pine needles as a substrate for gasification. Hydro Nepal J. Water, Energy Environ. 15, 73–81. https://doi.org/10.3126/hn.v15i0.11299.

Di Blasi, C., 2009. Combustion and gasification rates of lignocellulosic chars. Prog. Energy Combust 35, 121–140. https://doi.org/10.1016/j.pecs.2008.08.001.

Dong, J., Chi, Y., Tang, Y., Ni, M., Nzihou, A., Weiss-Hortala, E., Huang, Q., 2016. Effect of operating parameters and moisture content on municipal solid waste pyrolysis and gasification. Energy Fuel. 30, 3994–4001. https://doi.org/10.1021/acs.energyfuels.6b00042.

Double, J.M., Bridgwater, A.V., 1985. Sensitivity of Theoretical Gasifier Performance to System Parameters. In: V, W., Palz, J., Coombs, D.O.H. (Eds.), Energy from Biomass, Proceedings of the Third EC Conference, pp. 915–919.

Eke, J., Onwudili, J.A., Bridgwater, A.V., 2019. Influence of moisture contents on the fast pyrolysis of trommel fines in a bubbling fluidized bed reactor. Waste and Biomass Valorization. https://doi.org/10.1007/s12649-018-00560-2.

He, M., Xiao, B., Liu, S., Hu, Z., Guo, X., Luo, S., Yang, F., 2010. Syngas production from pyrolysis of municipal solid waste (MSW) with dolomite as downstream catalysts. J. Anal. Appl. Pyrolysis 87, 181–187. https://doi.org/10.1016/j.jaap.2009.11.005.

Holman, J.P., 2010. Heat Transfer, tenth ed. The McGraw-Hill Companies. https://doi.org/10.1603/EN11245 https://ec.europa.eu/energy/intelligent/projects/sites/ieeprojects/files/projects/documents/forest_standards_guide_en.pdf. (Accessed 6 August 2020).

https://www.cti2000.it/index.php?controller=pubblicazioni&action=show&id=15975. 2012, Accessed date (05/06/2020).

Kabalina, N., Costa, M., Yang, W., Martin, A., Santarelli, M., 2017. Exergy analysis of a polygeneration-enabled district heating and cooling system based on gasification of refuse derived fuel. J. Clean. Prod. 141, 760–773. https://doi.org/10.1016/j.jclepro.2016.09.151.

Karamarkovic, R., Karamarkovic, V., 2010. Energy and exergy analysis of biomass gasification at different temperatures. Energy 35, 537–549. https://doi.org/10.1016/j.energy.2009.10.022.

Kotas, T.J., 1985. Exergy analysis of simple processes. The Exergy Method of Thermal Plant Analysis 99–161. https://doi.org/10.1016/b978-0-408-01350-5.50011-8.

Kung, H.C., 1972. A mathematical model of wood pyrolysis. Combust. Flame 18, 185–195. https://doi.org/10.1016/S0010-2180(72)80134-2.

Lee, C.K., Chaiken, R.F., Singer, J.M., 1977. Charring pyrolysis of wood in fires by laser simulation. Symposium (International) on Combustion 16 (1), 1459–1470. https://doi.org/10.1016/S0082-0784(77)80428-1.

Li, G., Liu, Z., Liu, F., Yang, B., Ma, S., Weng, Y., Zhang, Y., Fang, Y., 2019. Advanced exergy analysis of ash agglomerating fluidized bed gasification. Energy Convers. Manag. 199 https://doi.org/10.1016/j.enconman.2019.111952.

Maa, P.S., Bailie, R.C., 1973. Influence of particle sizes and environmental conditions on high temperature pyrolysis of cellulosic material—i (theoretical). Combust. Sci. Technol. 7, 257–269. https://doi.org/10.1080/00102207308952366.

Nag, P.K., 2002. Power Plant Engineering, iiird ed. The Tata McGraw- Hill. https://doi.org/10.1007/978-1-4613-0427-2.

Prins, M.J., Ptasinski, K.J., Janssen, F.J.J.G., 2003. Thermodynamics of gas-char reactions: first and second law analysis. Chem. Eng. Sci. 58, 1003–1011. https://doi.org/10.1016/S0009-2509(02)00641-3.

Prins, M.J., Ptasinski, K.J., Janssen, F.J.J.G., 2006. Torrefaction of wood. Part 1. Weight loss kinetics. J. Anal. Appl. Pyrolysis 77, 28–34. https://doi.org/10.1016/j.jaap.2006.01.002.

Pyle, D.L., Zaror, C.A., 1984. Heat transfer and kinetics in the low temperature pyrolysis of solids. Chem. Eng. Sci. 39, 147–158. https://doi.org/10.1016/0009-2509(84)80140-2.

Rupesh, S., Muraleedharan, C., Arun, P., 2016. Energy and exergy analysis of syngas production from different biomasses through air-steam gasification. Front. Energy 1–13. https://doi.org/10.1007/s11708-016-0439-1.

Soto Veiga, J.P., Romanelli, T.L., 2020. Mitigation of greenhouse gas emissions using exergy. J. Clean. Prod. 260, 121092 https://doi.org/10.1016/j.jclepro.2020.121092.

Tang, L., Huang, H., 2005. Plasma pyrolysis of biomass for production of syngas and carbon adsorbent. Energy Fuel. 19, 1174–1178. https://doi.org/10.1021/ef049835b.

Tran, K.Q., Luo, X., Seisenbaeva, G., Jirjis, R., 2013. Stump torrefaction for bioenergy application. Appl. Energy 112, 539–546. https://doi.org/10.1016/j.apenergy.2012.12.053.